

Jing-Jing Xu<sup>1</sup>  
Mingrui An<sup>2</sup>  
Rui Yang<sup>2</sup>  
Jun Cao<sup>1</sup>  
Li-Hong Ye<sup>3</sup>  
Li-Qing Peng<sup>1</sup>

<sup>1</sup>College of Material Chemistry and Chemical Engineering, Hangzhou Normal University, Hangzhou, P. R. China

<sup>2</sup>Department of Surgery, University of Michigan Medical Center, Ann Arbor, MI, USA

<sup>3</sup>Department of Traditional Chinese Medicine, Hangzhou Red Cross Hospital, Hangzhou, P. R. China

Received January 13, 2016

Revised March 8, 2016

Accepted March 24, 2016

## Research Article

# Trace amounts of poly- $\beta$ -cyclodextrin wrapped carbon nanotubes for the microextraction of flavonoids in honey samples by capillary electrophoresis with light-emitting diode induced fluorescence detection

A novel dispersive micro-SPE method with trace poly- $\beta$ -CD wrapped multiwalled carbon nanotubes as sorbents was applied to extract flavonoids in honey samples. The analytes were then determined by CE with LED-induced fluorescence detection. The influencing parameters, such as the sorbent concentration, extraction time, and eluent type, were properly optimized. The established method had the advantages of simplicity, low consumption of sorbent amount (0.009 mg) and organic solvent (100  $\mu$ L), and high sensitivity, meeting the principle of green chemistry. Under the optimum conditions, the sorbents allowed the extraction and preconcentration of the flavonoids with enrichment factors in the range from 78 to 166. The recovery study performed at two different fortification levels provided an average recovery >91%. LODs for all the compounds ranged from 0.07 to 17.99 ng/mL. These results demonstrated that the proposed method could be used as a convenient and efficient extraction technique for analysis of flavonoids in different honey matrices.

### Keywords:

Dispersive micro-SPE / Flavonoids / Honey / LED-induced fluorescence detection / Poly- $\beta$ -CD wrapped carbon nanotubes  
DOI 10.1002/elps.201600016

## 1 Introduction

CDs are macrocyclic oligosaccharides including glucopyranose units linked by 1, 4-glucosidic bonds [1]. Given their hydrophobic inner cavity and hydrophilic outside surface, the special molecular structure of CDs can bind with various hydrophobic materials to form stable supramolecular host-guest complexes [2]. Thus, CDs are widely used in many fields, such as in drug delivery [3], electroanalysis [4], catalysis [5], and environmental protection [6]. Recently, poly- $\beta$ -CD has received a great deal of attention due to its unique physicochemical property and large surface. Poly- $\beta$ -CD as a highly water-soluble macromolecule is obtained by cross-linking  $\beta$ -CD with epichlorohydrin [7]. Moreover, poly- $\beta$ -CD molecule consists of many hydroxyl groups, which can ei-

ther react with the substrates or be used to selectively attach some functional groups.

Carbon nanotubes (CNTs), a new form of carbon atoms, are composed of graphene sheets rolled into seamless cylinders with different nanometer diameters and micrometer lengths [8]. They have seen various potential applications owing to their hydrophobicity, high electrical conductivity, and large specific surface area [9]. However, a major drawback for CNT utilization is their poor dispersion in aqueous solutions. As is well known, the conventional chemical modification strategies with concentrated H<sub>2</sub>SO<sub>4</sub>, HNO<sub>3</sub>, or other strong oxidizing agents tend to change the physicochemical nature of CNTs [10]. In order to overcome these defects, several noncovalent methods have been explored. Compared to covalent surface modification of CNTs, the noncovalent functionalization possesses the advantage of no disruption of the chemical structure and electronic property of the nanotubes [11]. The common materials linked noncovalently to the surface of CNTs, especially multiwalled CNTs (MWCNTs), are chitosan [12], CD [13], micelle [14], and polymer [15]. In recent years, some poly- $\beta$ -CD wrapped MWCNTs prepared by noncovalent modification methods have been reported. Moreover, these studies were mainly focused on the application in biosensing platform and supramolecular recognition fields, and the consumption of poly- $\beta$ -CD amount was considerable [7, 16]. To our knowledge, however, the

**Correspondence:** Dr. Jun Cao, College of Material Chemistry and Chemical Engineering, Hangzhou Normal University, Hangzhou 310036, China

**E-mail:** caojun91@163.com

**Fax:** +86-571-2886-7909

**Abbreviations:** CNT, carbon nanotube; CE-LED-IF, CE-LED-fluorescence detection; DLLME, dispersive liquid-liquid microextraction; DMSPE, dispersive micro-SPE; MSPE, magnetic SPE; MWCNT, multiwalled carbon nanotube

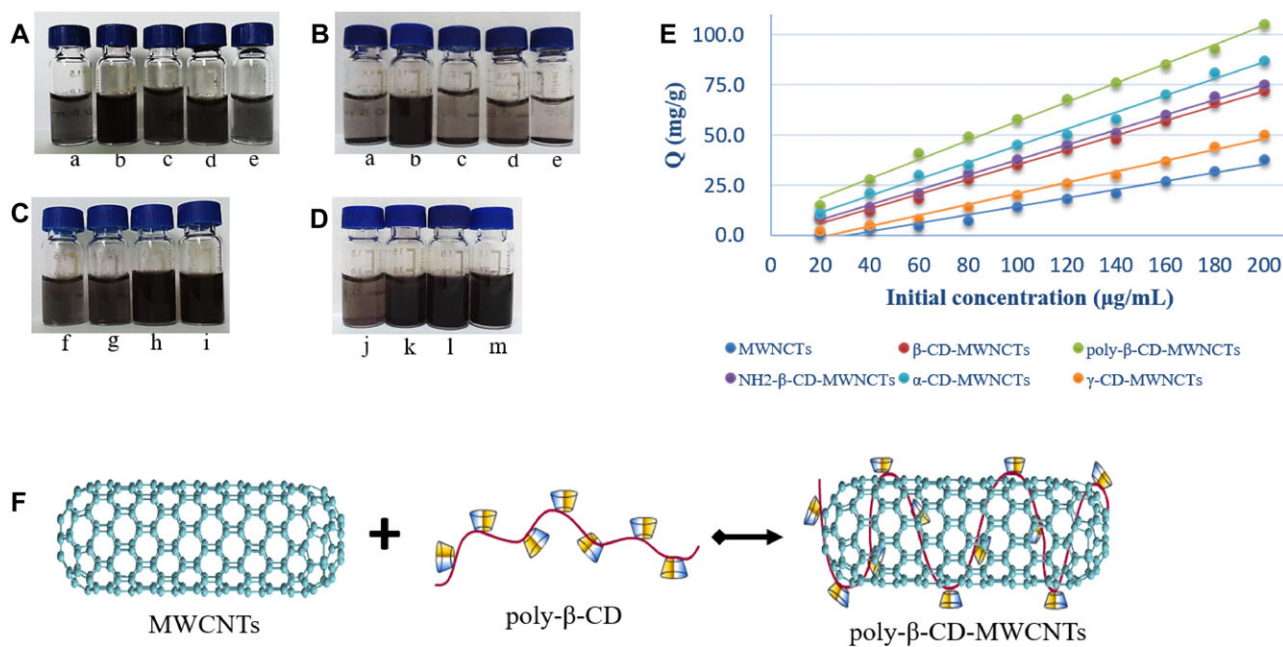


**Figure 1.** Pictures of (A) the type of CDs (a,  $\beta$ -CD; b, poly- $\beta$ -CD; c, NH<sub>2</sub>- $\beta$ -CD; d,  $\alpha$ -CD; e,  $\gamma$ -CD), (B) the type of CDs (taken 2 h after 2-min sonication), (C) the amount of poly- $\beta$ -CD (f, 0 mg; g, 0.5 mg; h, 1 mg; i, 2 mg), (D) the amount of MWCNTs (j, 0.5 mg; k, 1 mg; l, 2 mg; m, 4 mg). (E) Adsorption isotherms of CD-MWCNTs (a,  $\beta$ -CD; b, poly- $\beta$ -CD; c, NH<sub>2</sub>- $\beta$ -CD; d,  $\alpha$ -CD; e,  $\gamma$ -CD) and MWCNTs toward kaempferol, and (F) schematic illustration of poly- $\beta$ -CD functionalized MWCNTs.

poly- $\beta$ -CD-MWCNT composites for extraction of bioactive analytes from complex sample matrices have not been investigated.

Several sample-preparation techniques have been developed to extract analytes from various food matrices, such as magnetic SPE (MSPE) [17], dispersive micro-SPE (DMSPE) [18], matrix solid-phase dispersion [19], dispersive liquid-liquid microextraction (DLLME) [20], and SPE [21]. Among them, DMSPE is a miniaturization model of SPE that considerably reduces the consumption of sorbent amount and organic solvent, and simplifies the operation process. In this method, extraction is not carried out in a cartridge or column but in the bulk solution, which results in more rapidity and simplicity compared with the conventional SPE. In DMSPE, it is very important to select the most suitable sorbent material in order to improve the sensitivity of the process. The commonly used sorbents are silica [22], CNT [12], TiO<sub>2</sub> [23], and graphene [24]. However, no reports have been published on the application of trace poly- $\beta$ -CD-MWCNTs as sorbents in DMSPE.

Honey is a highly concentrated mixture of carbohydrates and often used as a natural preservative in many manufactured foods [25]. The main phytochemicals reported in honey samples are flavonoids (apigenin, galangin, kaempferol, luteolin, myricetin, and quercetin), phenolic acids (caffeic, chlorogenic, coumaric, gallic, homogentisic, syringic, and vanillic acids), and their derivatives [20]. However, recent studies reported that the antioxidant, antibacterial, anti-inflammatory, antithrombotic, and anti-allergic activities of honey are mainly attributed to the presence of flavonoids [26].

Therefore, identification and quantification of the flavonoids in honey matrices is of great interest. In this study, a novel DMSPE method using trace poly- $\beta$ -CD-MWCNTs as the sorbent was established for determination of flavonoids in honey samples by CE with LED-induced fluorescence detection (CE-LED-IF). In addition, the dispersion and characterization of poly- $\beta$ -CD-MWCNTs, experimental parameters including sorbent concentration, extraction time, diluent pH, and elution type were investigated in detail. The extraction method was expected to be widely applied for the analysis of phytochemicals in complex food matrices.

## 2 Materials and methods

### 2.1 Reagents and samples

ACN, methanol, and formic acid of HPLC grade were obtained from Sigma-Aldrich (St. Louis, MO, USA). Ethanol and *n*-propanol of analytical grade were from Hangzhou Chemical Reagent (Hangzhou, China).  $\beta$ -CD, poly- $\beta$ -CD, 3A-amino-3A-deoxy-(2AS,3AS)- $\beta$ -CD hydrate (NH<sub>2</sub>- $\beta$ -CD),  $\alpha$ -CD, and  $\gamma$ -CD were purchased from Tokyo Chemical Industry (Tokyo, Japan). MWCNTs (outer diameter (OD) 8–15 nm, length 0.5–2  $\mu$ m) were supplied by Nanjing XFNano Material Tech (Nanjing, China). All other chemicals were of analytical grade. The syringes (20 mL) were produced from Hangzhou Chemical Reagent (Hangzhou, China). Analytical standards of apigenin, luteolin, galangin, kaempferol, myricetin, and quercetin were purchased from Shanghai Winherb

Medical Technology (Shanghai, China) and stored in amber bottles. Wild chrysanthemum, acacia flower, and orange flower honey was supplied by local supermarket (Hangzhou, China). A standard mixture of six flavonoids at concentrations of 225 µg/mL for apigenin, 2000 µg/mL for luteolin, 25 µg/mL for galangin and kaempferol, 100 µg/mL for myricetin, and 50 µg/mL for quercetin was prepared in methanol and stored at 4°C.

## 2.2 Apparatus and CE-LED-IF

The detection system used for the adsorption-ability characterization of MWCNTs and poly-β-CD-MWCNTs was an Agilent model 1290 UHPLC with a UV detector (Agilent Technologies). The MWCNTs and poly-β-CD-MWCNTs were characterized by a SEM model Hitachi HT7700 (Tokyo, Japan). High-resolution transmission electron microscopy using an FEI Helios NanoLab 600 DualBeam microscope (FEI, the Netherlands) was performed at 200 kV. Ver551B atomic force microscope (AFM) was used to investigate the diameter of pristine MWCNTs and poly-β-CD-MWCNTs with silicon cantilevers “NSC15/AIBS” (µmash; NanoNavi, Japan). FTIR spectrum was used as a qualitative technique. The tested samples were combined with KBr powder and then pressed into a pellet. Finally, spectral range was 500 to 4000 cm<sup>-1</sup> with a Thermo Scientific Nicolet iS5 spectrometer (Madison, WI, USA).

The design of the CE-LED-IF system was reported previously [27]. In essence, an LED (Picometrics Technology Corporation; Labège, France; peak wavelength, 480 nm, spectral bandwidth, 25 nm; applied PM HV voltage, 650 V; rise time, 0.1 s) was employed as the excitation light source for fluorescence detection. The emission wavelength was obtained in the range of 510 to 760 nm. A 65 cm × 50 µm id (45 cm effective length) uncoated fused-silica capillary (Hebei Optical Fiber, China) was used for the separation, and the detection window was obtained by removing off a 6 mm of polyimide coating on the capillary.

For the first use, the capillary was preconditioned with 1.0 M NaOH for 10 min, 0.1 M NaOH for 10 min, and distilled water for 5 min. Prior to sample injection, the capillary was flushed with running buffer for 5 min. The buffer solution was 10 mM sodium borate, 8% methanol, and 2% 1-propanol. All chromatographic separation was executed at a voltage of 30 kV at 35°C. The samples were injected hydrodynamically for 3 s using 50 mbar of pressure. After each sample analysis, the capillary was flushed with 0.1 M NaOH for 3 min and running buffer for 3 min. In order to avoid the possible volatilization of methanol and obtain a good precision, the buffer solution was replaced after every two runs.

## 2.3 Sample preparation

Honey samples (3 g of each) were mixed with 6 mL of water (adjusted at pH 2 with concentrated HCl), and then subjected

to ultrasonication at 100 W (40 kHz) until they were completely dissolved (about 15 min). Finally, the fluid samples were filtered through 0.22-µm nylon filters prior to DMSPE.

## 2.4 Preparation of poly-β-CD-MWCNT suspension

MWCNTs were wrapped using poly-β-CD as a functionalization agent by applying Chen's soft cutting technique with minor modifications [28]. A 1 mg aliquot of poly-β-CD and 1 mg of raw MWCNTs were mixed and ground in an agate mortar and pestle system for 1 min. During the grinding time (1 min), 200 µL of water was added dropwise to form a sticky mixture. This blend was further ground without addition of water for 19 min to obtain a homogeneous black composite. Then, the composite was transferred to a glass vial and dispersed into 9.8 mL of water. Finally, the solution was sonicated for 2 min (100W, 40 kHz) to obtain a uniform poly-β-CD-MWCNTs suspension.

## 2.5 Characterization of adsorption performance

For investigation of the adsorption performance of poly-β-CD-MWCNT material, 1 mg poly-β-CD-MWCNTs or MWCNTs were equilibrated with 10 mL of a standard mixture of six flavonoids at concentrations of 20–200 µg/mL (only the data of kaempferol were given). It was mechanically shaken for 4 h at 100 × g, and then separated centrifugally (10 000 × g) for 10 min. Temperature was contained at 25°C in preliminary experiments. Residual flavonoids in the supernatant were detected by UHPLC, and the adsorption capacity ( $Q$ ) was calculated as following equation:

$$Q = (C_0 - C_e) V / M, \quad (1)$$

where  $C_0$  and  $C_e$  are the initial and equilibrium concentrations (µg/mL) of these six flavonoids,  $V$  is the volume of flavonoids solution (mL), and  $M$  is the mass of carbon materials (mg).

## 2.6 DMSPE procedure

The proposed extraction method was as follows: A 14.91 mL of aqueous solution containing 30 µL of the standard mixture or each honey sample was placed in a 30-mL glass vial. Next, 90 µL dispersed poly-β-CD-MWCNTs at a final concentration of 0.6 µg/mL were added. Subsequently, the vial was oscillated at maximum speed for 4 min, which promoted the interaction between the target analytes and solid-phase sorbents. After extraction, the whole volume (15 mL) was passed through a 0.22-µm disposable nylon filter (14 mm id) by an SPE device. The trace poly-β-CD-MWCNTs enriched with

the compounds were retained on the filter while the aqueous phase was discarded. Eventually, the filter was eluted with 100  $\mu$ L of methanol. The eluent was centrifuged at 13 000  $\times$  g for 3 min and injected into the CE-LED-IF equipment for further qualitative and quantitative analysis.

### 3 Results and discussion

#### 3.1 Dispersion of poly- $\beta$ -CD-MWCNTs in the water

Photographs of MWCNTs dispersed in water with different types of CD ( $\beta$ -CD, poly- $\beta$ -CD,  $\text{NH}_2$ - $\beta$ -CD,  $\alpha$ -CD, and  $\gamma$ -CD) are illustrated in Fig. 1A and B. These CDs possessing multifunctional groups and various physicochemical properties were observed with different capabilities of dispersing MWCNTs in the aqueous solutions (Fig. 1A and B (a–e)). As depicted in Fig. 1A, taken immediately after grinding and sonication, the functionalized MWCNTs ( $\beta$ -CD-MWCNTs, poly- $\beta$ -CD-MWCNTs,  $\text{NH}_2$ - $\beta$ -CD-MWCNTs,  $\alpha$ -CD-MWCNTs, and  $\gamma$ -CD-MWCNTs) were homogeneously dispersed in the water. However, only poly- $\beta$ -CD-MWCNTs exhibited good stability after 2 h standing (Fig. 1B). Evidently, the poly- $\beta$ -CD with more hydrophobic cavities than other CDs was strongly absorbed and entangled on the surface of raw MWCNTs by noncovalent interaction. The schematic illustration is demonstrated in Fig. 1F. Moreover, the stability and dispersibility of poly- $\beta$ -CD-MWCNTs composites was investigated by changing their concentrations in the aqueous solutions. Figure 1C shows that the color of MWCNTs darkened as the concentration of poly- $\beta$ -CD increased from 0 to 100  $\mu$ g/mL, because more MWCNTs in the water could be coated by higher concentration of poly- $\beta$ -CD. However, when the amount of poly- $\beta$ -CD was increased up to 200  $\mu$ g/mL, no significant difference in color was obtained. Figure 1D displays that increasing the concentration of MWCNTs in the aqueous solution (50 to 100  $\mu$ g/mL) resulted in a dispersion with deeper color (Fig. 1D (j and k)), but too large amount of MWCNTs in the water (200 to 400  $\mu$ g/mL) could aggregate together via the intermolecular interaction, and then caused a precipitation after standing for 2 h (data not shown). In addition, the adsorption performances of CD-MWCNTs ( $\beta$ -CD-MWCNTs, poly- $\beta$ -CD-MWCNTs,  $\text{NH}_2$ - $\beta$ -CD-MWCNTs,  $\alpha$ -CD-MWCNTs, and  $\gamma$ -CD-MWCNTs) and MWCNTs toward flavonoids at 20–200  $\mu$ g/mL are shown in Fig. 1E. The results showed that the amounts of kaempferol molecule adsorbed by the sorbent materials all increased with the kaempferol concentration increasing. However, poly- $\beta$ -CD-MWCNTs, compared with kinds of CD-MWCNTs, had a highest adsorption capacity for kaempferol. The use of poly- $\beta$ -CD, therefore, improved the adsorption ability of the MWCNTs. Taking into account the stability, dispersibility, adsorption capacity of poly- $\beta$ -CD-MWCNTs and the consumption of reagents, 1 mg of MWCNTs, 1 mg of poly- $\beta$ -CD, and 10 mL of water were used to prepare the sorbent in this study.

#### 3.2 Characterization of poly- $\beta$ -CD-MWCNTs

High-resolution transmission electron microscopy images of the poly- $\beta$ -CD-MWCNTs and pristine MWCNTs are shown in Fig. 2A and B. The average diameters of the pristine MWCNTs were 5–20 nm, clearly seen in Fig. 2A-(a). Compared with the outer diameters of pristine MWCNTs (Fig. 2A), a clear increase in nanotube diameters along the tube walls was observed after treatment with poly- $\beta$ -CD (Fig. 2B), and we could clearly observe that some of the poly- $\beta$ -CD was adhered onto the surface of MWCNTs (Fig. 2B(b)). To further investigate the poly- $\beta$ -CD distribution on the surface of MWCNTs, AFM imaging (see Fig. 3A–C) has allowed to characterize the morphology of the pristine and functionalized MWCNTs. From the images (Fig. 3B and C), the modification of MWCNTs with poly- $\beta$ -CD results in an enhancement of the lateral size of MWCNTs that is adequately appreciated in the section analysis where a higher height is distinct. Results of extensive height measurements (counting about 120 MWCNTs) indicate that the thicknesses of the poly- $\beta$ -CD that absorbed onto the surface of the MWCNTs were at least 5–10 nm (counting about 100 MWCNTs). Additionally, the morphology of the MWCNTs before and after wrapped by poly- $\beta$ -CD was characterized by SEM (Fig. 2C and D). It was clear that the raw MWCNTs were in bundles with an unordered arrangement (Fig. 2C). When poly- $\beta$ -CD was used to disperse MWCNTs, the obtained composite was much thicker than the untreated MWCNTs (Fig. 2D). These observations were in full agreement with the previous study [7].

Figure 2E displays the FTIR spectra of pristine MWCNTs (curve a), poly- $\beta$ -CD (curve b), and poly- $\beta$ -CD-MWCNTs (curve c). In curve c, it was found that the poly- $\beta$ -CD-MWCNTs exhibited some typical absorption features of the poly- $\beta$ -CD, such as the C–O and C–O–C stretching vibrations of glucose units at 1026  $\text{cm}^{-1}$  and 1152  $\text{cm}^{-1}$ ,  $\text{CH}_2$  stretching vibrations at 2919  $\text{cm}^{-1}$ , and C–H bending vibrations at 1430  $\text{cm}^{-1}$ . A strong band caused by O–H stretching vibration was seen at 3440  $\text{cm}^{-1}$ , which further confirmed the presence of hydroxyl groups of poly- $\beta$ -CD combined with CNTs. In addition, the peaks around 1600  $\text{cm}^{-1}$  of poly- $\beta$ -CD and poly- $\beta$ -CD-MWCNTs were corresponding to the vibration of the remaining  $\text{H}_2\text{O}$ . The FTIR analysis demonstrated that all main functional groups in MWCNTs and poly- $\beta$ -CD were presented in the final functionalized sorbents, only with a slight decrease in the wavenumber when conjugated to each other [7, 29].

#### 3.3 Structure-fluorescence relationships

Absorption spectra of flavonoids in the buffer solution were investigated in this work and the results are shown in Fig. 4A. In the range of 350–500 nm, these compounds exhibited characteristic peaks located at 384–392 nm, which were used as the excitation wavelength for measuring the fluorescence intensities. The interaction of flavonoids with the 10 mM sodium borate system was further studied by the fluorescence method.

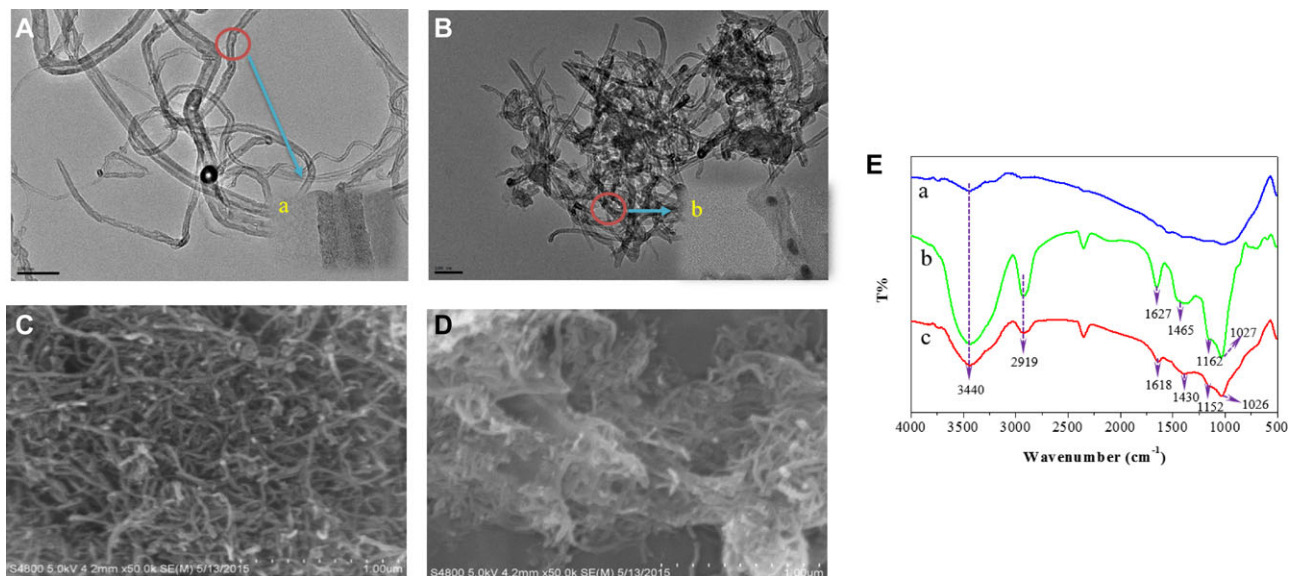


**Figure 2.** Transmission electron microscopy images (A, B) and SEM images (C, D) of MWCNTs and poly- $\beta$ -CD-MWCNTs ((a) and (b) were MWCNTs and poly- $\beta$ -CD-MWCNTs magnification), and FTIR spectra (E) of MWCNTs (a), poly- $\beta$ -CD (b), and poly- $\beta$ -CD-MWCNTs (c).

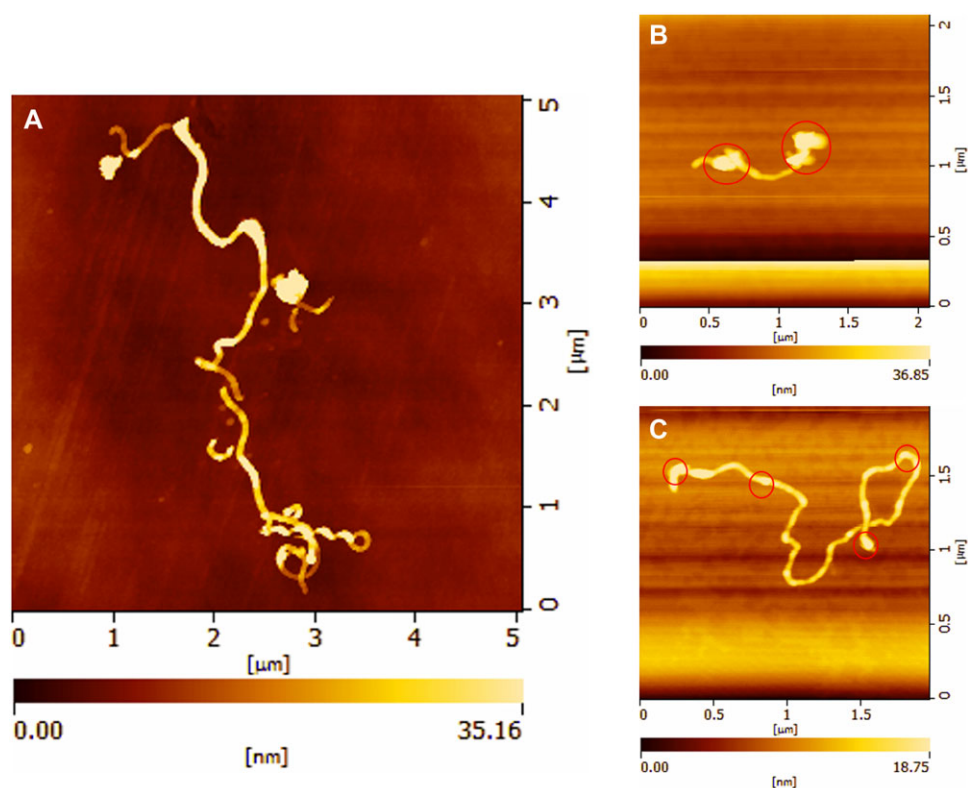


**Figure 3.** AFM images of pristine MWCNTs (A) and poly- $\beta$ -CD-MWCNTs (B).

When the target analytes were dissolved in the alkaline buffer, their relative fluorescences were significantly improved with a large red shift compared with the solutes in methanol (data not shown). This could be ascribed to the extended  $\pi$  conjugation of the flavonoid molecules. As illustrated in Fig. 4B, compared to the flavones (apigenin, luteolin) lacking the  $-\text{OH}$  groups in the C rings ( $\lambda_{\text{em}} \approx 510$  nm), flavonols (galangin,

kaempferol, myricetin, and quercetin) possessing 3-OH substituents had larger maximum emission wavelength values ( $\lambda_{\text{em}} \approx 550$  nm). The possible reasons were as follows: (i) it was known that the H-bond between C = O and 5-OH would facilitate the nonradiative deactivation while that between the carbonyl and the hydroxy group at the 3-position could enhance the excited-state proton transfer process [27, 30]; (ii)

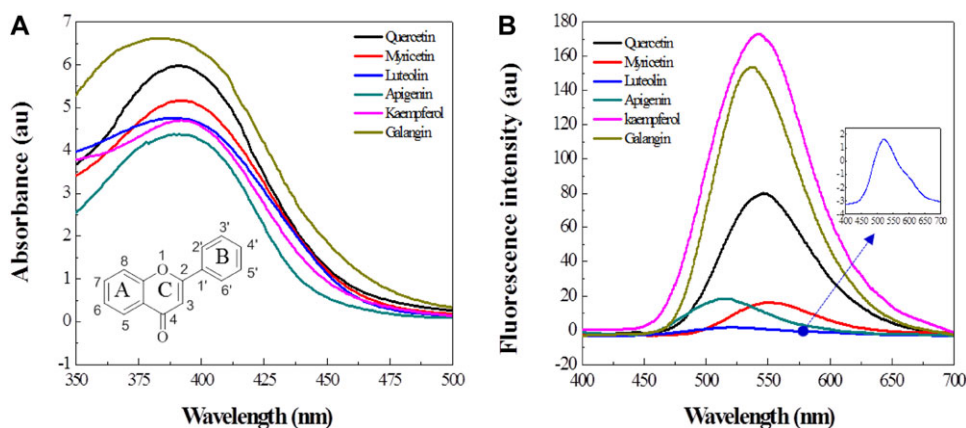


**Figure 4.** Absorption spectra (A) and fluorescent emission spectra (B) of analytes in the presence of running buffer.

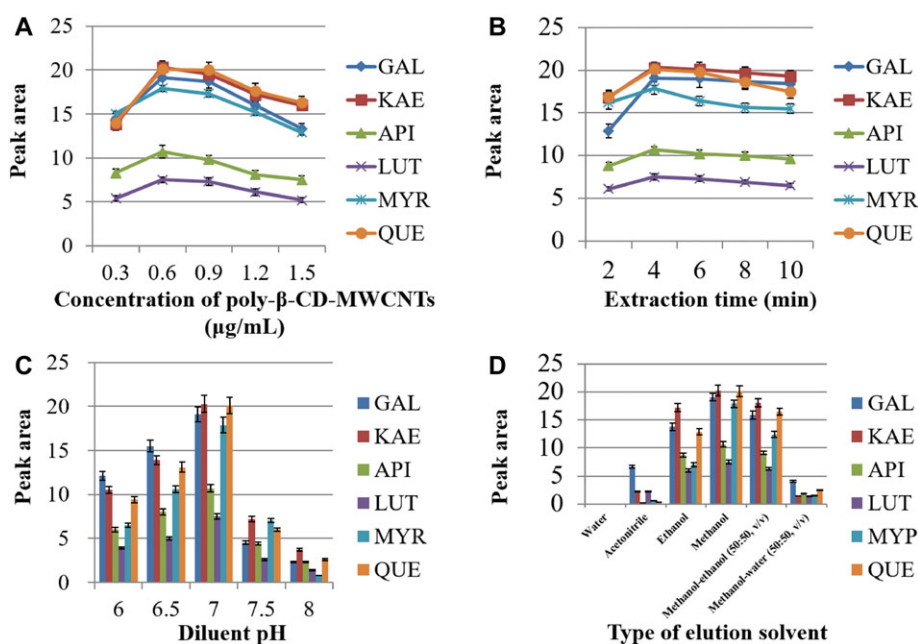


**Figure 5.** The optimization of DMSPE process. Extraction conditions: standard mixture volume, 30  $\mu\text{L}$ ; aqueous mixture volume, 15 mL; sorbent material, poly- $\beta$ -CD-MWCNTs; elution volume, 100  $\mu\text{L}$ . Analytes: (1) galangin (GAL), (2) kaempferol (KAE), (3) apigenin (API), (4) luteolin (LUT), (5) myricetin (MYR), (6) quercetin (QUE). (A) Effect of the sorbent concentration on the extraction efficiency of flavonoids. (B) Effect of the extraction time. (C) Effect of the diluent pH. (D) Effect of the type of elution solvent.

the 5-OH group in the vibrationally excited molecule brought a motion to convert its H-bond from an intramolecular to an intermolecular one, and then activated the 3-OH intramolecular proton transfer fluorescence [30]. Therefore, it was confirmed that the flavonoid structures had a remarkable impact on the interaction between analytes and the buffer solution, and then affected their fluorescence responses. Additionally, the filter of LED-IF stopped the emission wavelength before 510 nm and transmitted the  $\lambda_{\text{em}}$  higher than 510 nm until 760 nm, which resulted in relatively weaker fluorescence responses for apigenin and luteolin (Fig. 5).

### 3.4 Optimization of DMSPE procedure

To achieve the best extraction efficiency of flavonoids, several influencing parameters (i.e., the concentration of sorbent, extraction time, diluent pH, and eluent type) were systematically explored.

#### 3.4.1 Effect of sorbent concentration

To explore the effect of the concentration of poly- $\beta$ -CD-MWCNTs on the extraction efficiency of the six flavonoids, different concentrations of the sorbent, ranging from 0.3 to 1.5  $\mu\text{g}/\text{mL}$ , were carefully studied under the following conditions: aqueous solution, 15 mL; spiked standard mixture, 30  $\mu\text{L}$ ; pH, 7; extraction time, 4 min; and eluent type, methanol. As shown in Fig. 5A, it was found that the peak areas of the compounds were increased with increasing the concentration of poly- $\beta$ -CD-MWCNTs up to 0.6  $\mu\text{g}/\text{mL}$ . To the best of our knowledge, the poly- $\beta$ -CD possessed various interactions with the flavonoid compounds. The common binding forces involved in this complex formation are hydrogen bonding between the phenolic hydroxyls of the target analytes and the hydroxyl groups of the poly- $\beta$ -CD and hydrophobic interactions between the hydrophobic moiety of the flavonoid molecules and the poly- $\beta$ -CD cavities. Moreover, van der Waals force and  $\pi$ - $\pi$  stacking between the

**Table 1.** Linear regression data, repeatability, reproducibility, LODs, and LOQs of the investigated compounds

Analytes	Calibration curve	$r^2$	Intraday repeatability (n = 6)		Interday reproducibility (3 days)		Reproducibility between samples (n = 3, RSD%)		LOD (ng/mL)		LOQ (ng/mL)	
			Migration times	Peak areas	Migration times	Peak areas	Migration times	Peak areas	No enrichment	After enrichment	No enrichment	After enrichment
			times	areas	times	areas	times	areas	enrichment	enrichment	enrichment	enrichment
Galangin	Pure solvent	$y = (0.2279 \pm 0.0183)x - (0.1994 \pm 0.0871)$	0.54	3.08	2.21	3.62	2.56	4.16	14.93	0.09	0.3	
	Matrix-matched solvent	$y = (0.2438 \pm 0.0227)x - (0.1864 \pm 0.0950)$	0.9997									
Kaempferol	Pure solvent	$y = (0.2391 \pm 0.0095)x - (0.1918 \pm 0.0752)$	0.59	2.74	1.53	3.81	2.63	2.06	11.04	0.07	0.25	
	Matrix-matched solvent	$y = (0.2421 \pm 0.0139)x - (0.2395 \pm 0.0672)$	0.9981									
Apigenin	Pure solvent	$y = (0.0168 \pm 0.0085)x - (0.0516 \pm 0.0027)$	0.88	1.83	2.02	2.47	2.64	5.31	127.44	1.02	3.21	
	Matrix-matched solvent	$y = (0.0173 \pm 0.0093)x - (0.0601 \pm 0.0041)$	0.9993									
Luteolin	Pure solvent	$y = (0.0024 \pm 0.0011)x - (0.4225 \pm 0.0179)$	1.04	3.66	1.02	4.06	3.53	2.07	1919.85	17.99	53.97	
	Matrix-matched solvent	$y = (0.0025 \pm 0.0016)x - (0.4951 \pm 0.0543)$	0.9924									
Myricetin	Pure solvent	$y = (0.0355 \pm 0.0027)x - (0.2016 \pm 0.0074)$	0.74	2.5	1.79	3.61	2.62	4.2	46.52	0.6	2.02	
	Matrix-matched solvent	$y = (0.0324 \pm 0.0027)x - (0.2497 \pm 0.323)$	0.9967									
Quercetin	Pure solvent	$y = (0.1066 \pm 0.0823)x - (0.1955 \pm 0.0427)$	0.81	3.83	0.85	2.44	2.59	4.99	33.65	0.22	0.67	
	Matrix-matched solvent	$y = (0.1047 \pm 0.0758)x - (0.1819 \pm 0.0564)$	0.9987									

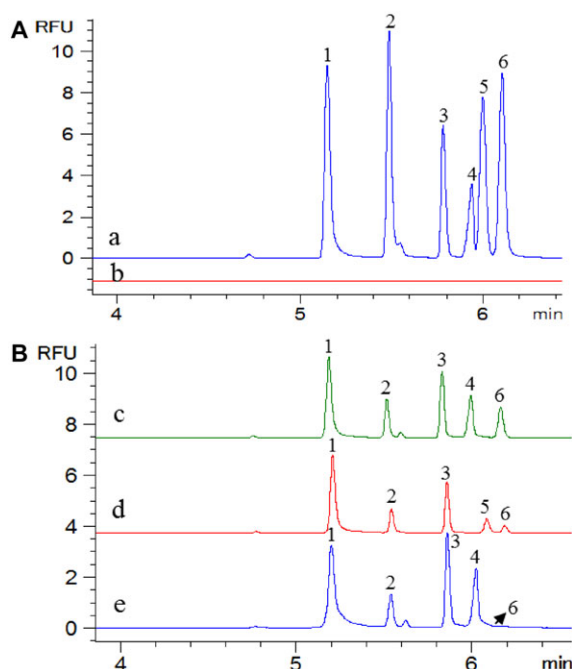


**Figure 6.** Typical electropherograms of standard mixture (A: a, after DMSPE; b, without DMSPE) and samples (B: c, orange flower honey; d, acacia flower honey; e, wild chrysanthemum honey) under the optimum conditions.

$\pi$  orbitals of MWCNTs and those of the phenyl groups presented in flavonoids had an important effect on improving the extraction efficiency. However, when higher concentrations of sorbent (0.9–1.5  $\mu\text{g}/\text{mL}$ ) were employed in the extraction, the extraction yields for all the analytes slightly decreased due to the increased difficulty in the elution process. To obtain the best results, 0.6  $\mu\text{g}/\text{mL}$  of poly- $\beta$ -CD-MWCNTs was chosen as the optimal concentration.

### 3.4.2 Effect of extraction time

It is well known that oscillating process is an effective way to promote mass transfer from aqueous phase to the active sites of extracting phase. In order to achieve the highest extraction efficiency of analytes, the extraction time was investigated in the range of 2–10 min. Other experimental conditions were the same as above. The results indicated that the peak areas were increased as the extraction time varied from 2 to 4 min (Fig. 5B). Presumably, the extraction time played a significant impact on the partition of target compounds between aqueous phase and poly- $\beta$ -CD-MWCNTs. When the oscillating time was extended, the interactions between the analytes and the sorbents were increased due to the large surface area of MWCNTs and the unique properties of poly- $\beta$ -CD. This phenomenon also illustrated that the equilibrium-driven process was easy to achieve within a short extraction time. However, the extraction performances of all the tested compounds slightly decreased after 4 min extraction. This

occurrence might be due to the back extraction of analytes from sorbent into aqueous solution [31]. Therefore, a duration of 4 min was employed as the optimum extraction time.

### 3.4.3 Effect of diluent pH

The pH of the sample solution is one of the most crucial factors in DMSPE optimization by influencing both the existing forms and charge densities on the surface of the compounds. In this study, the effect of the diluent pH on extraction efficiency was investigated over the pH range from 6 to 8 by adding 1 M HCOOH or 0.1 M NaOH into the aqueous solution. According to the results in Fig. 5C, pH values lower than 7 gave relatively poor analyte enrichment, while the peak areas of the six flavonoids sharply decreased when the diluent pH was beyond 7. For this phenomenon, it might be the reason that the flavonoids and poly- $\beta$ -CD would be ionized at pH values lower than their  $pK_a$  values ( $pK_a = 6.4$ – $6.9$  for six analytes,  $pK_a = 12.2$  for poly- $\beta$ -CD), and then the hydrogen bonding,  $\pi$ - $\pi$  stacking, and electrostatic interaction between the sorbent and the target analytes were decreased. In addition, a decrease of hydrophobicity of the compounds had occurred when the pH value of the sample solution was greater than 7, which would prevent the access of flavonoid compounds to the adsorption sites on the poly- $\beta$ -CD-MWCNTs surface. As a result, a pH value of 7 was selected for all the subsequent experiments.

### 3.4.4 Effect of elution type

To choose the best eluent for desorbing analytes from the sorbent, four common polar solvents and two mixed solvents including water, ACN, ethanol, methanol, methanol–ethanol (50:50, v/v), and methanol–water (50:50, v/v) were examined. For convenience, the volume of the six solvents was fixed at 100  $\mu\text{L}$ . The results in Fig. 5D-(a) indicate that no compounds were eluted off the nylon filter when using water as the elution solvent. This might result from the hydrophobicity of the organic flavonoids. Moreover, compared with single solvents (ethanol and water), the mixed solvents (methanol–ethanol (50:50, v/v) and methanol–water (50:50, v/v)) gave better desorption results in terms of peak areas of analytes (Fig. 5D-(e and f)). The highest extraction efficiency for all the analytes was obtained after washing with methanol. The strong interactions between the solutes and methanol could be attributed to the hydrogen bonding and small steric hindrance. Based on the above discussion, methanol was chosen as the desorption solvent.

## 3.5 Analytical figures of merit

The linearity, repeatability, reproducibility, LOD, and limit of quantification (LOQ) were evaluated under optimum conditions (Table 1). A series of calibration standards were



**Table 2.** The concentration and recovery of samples

Analytes	Wild chrysanthemum honey (ng/mL)	Acacia flower honey (ng/mL)	Orange flower honey (ng/mL)	Average recovery <sup>a)</sup> (% , <i>n</i> = 3)	ME (RSD, %)
Galangin	48.26	31.15	32.47	95 ± 2.2	99 (5)
Kaempferol	12.09	7.49	11.68	97 ± 1.6	109 (4)
Apigenin	413.79	193.55	259.02	103 ± 3.6	111 (4)
Luteolin	2426.04	—	1592.71	91 ± 3.9	96 (2)
Myricetin	—	36.66	—	99 ± 4.2	107 (5)
Quercetin	2.72	6.81	25.29	101 ± 3.8	113 (3)

a) Mean ± SD.

prepared in the range 1.00–3000.00 ng/mL. Calibration curves of analytes were established by plotting the peak areas of flavonoids versus their concentrations in pure solvent as well as in matrix-matched standards solutions. A good linearity was obtained throughout the concentration range with the correlation coefficient ( $r^2$ ) >0.99. The precision of the instrument was evaluated by measuring intraday repeatability and interday reproducibility by replicate injection of a standard mixture. Intraday precision was assessed by analyzing six continuous injections in one day, and the calculated RSD values of migration times and peak areas were over the range 0.54–1.04% and 1.83–3.83%. Interday precision was generated on three consecutive days with RSDs of migration times and analyzed peak areas in the range 0.85–2.21% and 2.44–4.06%. Reproducibility between samples was executed three times in parallel to evaluate the proposed method. The results showed that the RSD values of the migration times and the peak areas were less than 3.53 and 5.31%. These results met the validation acceptance criteria. The LOD and LOQ were defined as the lowest concentration on the calibration curves yielding a *S/N* ratio of 3 and 10, respectively. In DMSPE, the LOD and LOQ for six flavonoids ranged from 0.07 to 17.99 ng/mL and from 0.25 to 53.97 ng/mL, respectively. Furthermore, the enrichment factor, which was calculated by comparing the LOD values of the tested compounds before and after the DMSPE process, was 78–166.

### 3.6 Sample analysis

In order to evaluate the applicability of the proposed method for real samples, an attempt was made to determine flavonoids in different honey samples (wild chrysanthemum, acacia flower, and orange flower honey). The main chromatograms of standards and real honey samples are shown in Fig. 6, and the contents of six flavonoids are listed in Table 2. The results indicated that these samples were found with target analytes at concentrations of 2.72–2426.04 ng/mL. The recovery was assessed by spiking specified amount of standards at two concentration levels (1 and 50 ng/mL for galangin, kaempferol, and quercetin; 5 and 300 ng/mL for

apigenin and myricetin; 60 and 2000 ng/mL for luteolin) to three honey samples (15-mL aqueous solutions consisted of 14.85 mL water, 30  $\mu$ L of standard solutions, and 30  $\mu$ L of samples and 90  $\mu$ L of sorbents). The values were calculated by the following formula: recovery (%) = 100  $\times$  (collected concentration – initial concentration)/spiked concentration. The average recovery was in the range 91 to 103% with SD values from 1.6 to 4.2%. Matrix effect (ME, %) was assessed by comparing responses of target standards in aqueous solvent and honey matrix (the honey matrix using a solution with high concentration of fructose and glucose). The ME values were calculated as follows: ME (%) = Slope of flavonoids after extraction spike/slope of flavonoids in standard solution  $\times$  100. The ME values were in the range 96 to 113%, which meant that the matrices had little effect on the extraction of flavonoids by DMSPE step in this work. These analytical results showed that the established method was feasible and reliable for the analysis of real samples.

### 3.7 Comparison of DMSPE with previously reported methods

A comparison of the proposed method with other counterparts based on the use of SPE, DMSPE (other matrices), and DLLME is presented in Table 3. The comparison was carried out on the basis of different instrumental techniques, some operational (extraction solvent, sorbent amount, and elution solvent) and analytical (LOD and recovery) properties. As can be seen in Table 3, DMSPE provided better sensitivity (0.07–17.99 ng/mL) for target compounds by using lower sorbent amount (0.009 mg) and elution solvent volume (100  $\mu$ L) than that of SPE and DMSPE. These performance characteristics are of great interest for the routine laboratories in the trace analysis of flavonoids. In addition, compared with ACN, chloroform, EDTA–McIlvaine buffer and phosphate used in DLLME and others DMSPE, water as the extraction solvent used in the present method possessed the merit of lower toxicity. Therefore, it could be concluded that our proposal using poly- $\beta$ -CD-MWCNTs as sorbent was a sensitive and green method for the determination of flavonoids in honey matrices.

Table 3. Comparison of DMSPE with previously reported methods

Analytes	Matrix	Instrumental technique	Extraction technique	Soebent amount (mg)	Extraction solvent	Elution type and volume	LOD (ng/mL)	Recovery (%)	Reference
Quercetin, kaempferol	Linden honey, heather honey	HPLC-UV	SPE	2500	Water	Methanol, 50 mL	30–60	40.0–85.4	[32]
Quercetin	Citrus honey	HPLC-UV	SPE	500	Water	Water/methanol (87:13, v/v), 10 mL	222	90.7	[33]
Myricetin, luteolin, apigenin, kaempferol	Acacia, linden, chestnut, fir, spruce, floral and forest honey	LC-DAD-ESI/MS	SPE	200	Water	Methanol:ACN (2:1, v/v), 3 mL	—	94.3–104.5	[25]
Myricetin, quercetin, kaempferol	Lavender, orange blossom, rosemary, heather, eucalyptus, chestnut, thyme and flowers honey	LC-DAD	DLLME	—	ACN, chloroform	—	0.7–4.1	80–111	[26]
Myricetin, luteolin, apigenin, kaempferol, quercetin, galangin	CH1–CH3 acacia, CH4–5 sulla, CH6 thistle, CH7 citrus honey	HPLC-UV	DLLME	—	Chloroform	—	160–660	20.3–99.4	[34]
Bisphenol A	Whole, defatted, and skim milks	HPLC-UV	DMSPE	80	EDTA–Mclvaine buffer/ACN solution (20/80, v/v)	Methanol, 500 $\mu$ L	3.05	86–99	[35]
Oxacillin, cloxacillin, dicloxacillin	Six commercial milks	HPLC-UV	DMSPE	75	100 mM phosphate buffer and water	Methanol, 100 $\mu$ L	2.0–3.3	80.3–99.5	[36]
Lomefloxacin and ofloxacin	Plasma and urine	SPE-enhanced spectrofluorimetry	DMSPE	25	Water	Methanol, 1 mL	12–15	92–99	[37]
Myricetin, luteolin, apigenin, kaempferol, quercetin, galangin	Wild chrysanthemum, acacia flower, and orange flower honey	CE-LED-IF	DMSPE	0.009	Water	Methanol, 100 $\mu$ L	0.07–17.99	91–103	This method

## 4 Concluding remarks

In this work, a convenient and rapid DMSPE method coupled with CE-LED-IF detection was developed for the extraction and preconcentration of flavonoids from honey samples. The poly- $\beta$ -CD wrapped MWCNTs were applied for the first time as solid-phase sorbents, and they not only increased the extraction efficiency of the target compounds due to the existence of hydrogen bonding interaction between sorbent and analytes, but also improved stability of the MWCNTs and their dispersibility in aqueous solutions. Compared with conventional SPE and DLLME methods, this approach was more environmentally friendly, and could greatly reduce the consumption of organic solvent and sorbent amount and improve sensitivity. Moreover, the proposed method offered low LODs, good precision, acceptable recovery, and high enrichment factor. The results indicated that this proposal was simple, green, and practically feasible for the routine analysis of flavonoids in various complex honey samples.

*This study was supported by National Natural Science Foundation of China (No.81274065), Zhejiang Provincial Natural Science Foundation of China (LY15H280016), Hangzhou social development of scientific research projects (No. 20150533B05), Research on Public Welfare Technology Application Projects of Zhejiang Province (No. 2014C37069), Young and Middle-Aged Academic Leaders of Hangzhou (2013-45), and the new-shoot Talents Program of Zhejiang province (2015R423070).*

*The authors have declared no conflict of interest.*

## 5 References

- Mura, P., *J. Pharm. Biomed. Anal.* 2014, **101**, 238–250.
- Xue, J., Jia, Z., Jiang, X., Wang, Y., Chen, L., Zhou, L., He, P., Zhu, X., Yan, D., *Macromolecules* 2006, **39**, 8905–8907.
- Mura, P., Bragagni, M., Mennini, N., Cirri, M., Maestrelli, F., *Int. J. Pharm.* 2014, **475**, 306–314.
- Li, J. P., Wu, X. Z., Yu, Y., Le, S. W., *J. Solid State Electrochem.* 2009, **13**, 1811–1818.
- Rostamnia, S., Doustkhah, E., *J. Magn. Magn. Mater.* 2015, **386**, 111–116.
- Ferey, L., Delaunay, N., Rutledge, D. N., Cordella, C. B. Y., This, H., Huertas, A., Raoul, Y., Gareil, P., *Talanta* 2014, **119**, 572–581.
- Zhang, W., Chen, M., Gong, X. D., Diao, G. W., *Carbon* 2013, **61**, 154–163.
- Yan, Y. B., Miao, J. W., Yang, Z. H., Xiao, F. X., Yang, H. B., Liu, B., Yang, Y. H., *Chem. Soc. Rev.* 2015, **44**, 3295–3346.
- Yang, L., Fan, S. M., Deng, G. G., Li, Y. C., Ran, X., Zhao, H., Li, C. P., *Biosens. Bioelectron.* 2015, **68**, 617–625.
- Grassi, G., Scala, A., Piperno, A., Iannazzo, D., Lanza, M., Milone, C., Pistone, A., Galvagno, S., *Chem. Commun.* 2012, **48**, 6836–6838.
- Pang, J. Y., Xu, G. Y., Bai, Y., Yuan, S. L., He, F., Wang, Y. J., Sun, H. Y., Hao, A. Y., *Comput. Mater. Sci.* 2010, **50**, 283–290.
- Cao, W., Hu, S. S., Ye, L. H., Cao, J., Xu, J. J., Pang, X. Q., *J. Chromatogr. A* 2015, **1390**, 13–21.
- Iannazzo, D., Mazzaglia, A., Scala, A., Pistone, A., Galvagno, S., Lanza, M., Riccucci, C., Ingo, G. M., Colao, I., Sciortino, M. T., Valle, F., Piperno, A., Grassi, G., *Colloids Surface B Biointerfaces* 2014, **123**, 264–270.
- Lin, J. F., Mason, C. W., Adame, A., Liu, X., Peng, X. H., Kannan, A. M., *Electrochim. Acta* 2010, **55**, 6496–6500.
- Rao, W., Cai, R., Yin, Y. L., Long, F., Zhang, Z. H., *Talanta* 2014, **128**, 170–176.
- Yang, H. P., Zhu, Y. F., Chen, D. C., Li, C. H., Chen, S. G., Ge, Z. C., *Biosens. Bioelectron.* 2010, **26**, 295–298.
- Hu, S. S., Cao, W., Dai, H. B., Da, J. H., Ye, L. H., Cao, J., Li, X. Y., *J. Agric. Food Chem.* 2014, **62**, 8822–8829.
- Jiménez-Soto, J. M., Cárdenas, S., Valcárcel, M., *Anal. Chim. Acta* 2012, **714**, 76–81.
- Cao, W., Hu, S. S., Ye, L. H., Cao, J., Pang, X. Q., Xu, J. J., *Food Chem.* 2016, **190**, 474–480.
- Campone, L., Piccinelli, A. L., Pagano, I., Carabetta, S., Sanzo, R. D., Russo, M., Rastrelli, L., *J. Chromatogr. A* 2014, **1334**, 9–15.
- Stafiej, A., Pyrzynska, K., *Microchem. J.* 2008, **89**, 29–33.
- Galán-Cano, F., Lucena, R., Cárdenas, S., *Microchem. J.* 2013, **106**, 311–317.
- García-Valverde, M. T., Lucena, R., Galán-Cano, F., Cárdenas, S., Valcárcel, M., *J. Chromatogr. A* 2014, **1343**, 26–32.
- Kocot, K., Leardi, R., Walczak, B., Sitko, R., *Talanta* 2015, **134**, 360–365.
- Bertoncelj, J., Polak, T., Kropf, U., Korošec, M., Golob, T., *Food Chem.* 2011, **127**, 296–302.
- Campillo, N., Viñas, P., Férrez-Melgarejo, G., *Talanta* 2015, **131**, 185–191.
- Cao, W., Hu, S. S., Li, X. Y., Pang, X. Q., Cao, J., Ye, L. H., Dai, H. B., Liu, X. J., Da, J. H., Chu, C., *J. Chromatogr. A* 2014, **1358**, 277–284.
- Chen, J., Dyer, M. J., Yu, M. F., *J. Am. Chem. Soc.* 2001, **123**, 6201–6202.
- Chen, M., Meng, Y., Zhou, J., Diao, G. W., *J. Power Sources* 2014, **265**, 110–117.
- Liu, W., Guo, R., *Colloid Surface A* 2006, **274**, 192–199.
- See, H. H., Sanagi, M. M., Wan Ibrahim, W. A., Naim, A. A., *J. Chromatogr. A* 2010, **1217**, 1767–1772.
- Michalkiewicz, A., Biesaga, M., Pyrzynska, K., *J. Chromatogr. A* 2008, **1187**, 18–24.
- Hadjmohammadi, M. R., Nazari, S., Kamel, K., *Chromatographia* 2009, **69**, 1291–1297.
- Song, X. Y., Ha, W., Chen, J., Shi, Y. P., *J. Chromatogr. A* 2014, **1374**, 23–30.
- Reyes-Gallardo, E. M., Lucena, R., Cárdenas, S., *Microchem. J.* 2016, **124**, 751–756.
- Yahaya, N., Sanagi, M. M., Mitome, T., Nishiyama, N., Ibrahim, W. A. W., Nur, H., *Food Anal. Methods* 2015, **8**, 1079–1087.
- Amoli-Diva, M., Pourghazi, K., Hajjaran, S., *Mater. Sci. Eng. C Mater. Biol. Appl.* 2016, **60**, 30–36.